OBSERVATIONS OF A SEVERE HAIL-BEARING STORM BY AN OPERATIONAL X-BAND POLARIMETRIC RADAR IN THE MEDITERRANEAN AREA

246

Gianfranco Vulpiani[1] * and Luca Baldini[2]
[1] Department of Civil Protection, Presidency of the Council of Ministers, Rome, Italy
[2] Institute of Atmospheric Sciences and Climate, National Research Council, Rome, Italy

1. INTRODUCTION

Several experimental studies undertaken in the last decade have outlined the benefit of dual-polarization techniques in compensating the major limitation on the use of X-band radars for heavy precipitation measurements (e.g., Matrosov et al., 2005; Anagnostou et al., 2008; Anagnostou et al., 2010), i.e., attenuation. Taking advantages from differential phase measurements, it is either possible to compensate attenuation or to improve rainfall estimates, especially in heavy precipitation regimes (Wang and Chandrasekar, 2011). However, despite the generally comforting results in rainfall amount and Raindrop Size Distribution (RSD) retrieval, it is trivial to state that any attenuation correction technique cannot overtake the physical limit represented by signal extinction, that can be considered as the main limitation on the quantitative use of a stand-alone X-band radar for operational purposes that can be mitigated by resorting to a proper network design (Junyent and Chandrasekar, 2009).

In Matrosov et al. (2013), the utility of X-band polarimetric radar observations for convective-rainfall estimations in presence of rain-hail mixture was explored. The authors confirmed the benefit on the use of phase-based algorithms, they being "uncontaminated" by dry hailstones, due to the spherical-like appearance related to tumbling fall mode. Generally speaking, the presence of hail enhances scattering and absorption processes at microwaves, increasing reflectivity and attenuation.

According to Rasmussen and Heymsfield (1987), a torus of water forms around the melting hailstones, leading to a pseudo-stable non-tumbling fall mode. Consequently, the polarimetric signature of melting hail can be characterized by positive differential reflectivity and differential phase shift, depending on size and water coat thickness. At C-band, Tabary et al. (2009), attributed the huge observed differential attenuation to wet hail, confirming the water torus hypothesis.

This work is aimed at documenting the effects of rain-hail mixture on the polarimetric radar signatures analyzing a strong convective precipitation event, flash flooding the city of Catania (Sicily), Italy, observed by the operational X-band weather radar located in the nearby airport. Absolute and differential attenuation are dealt with differential phase measurements properly processed through an iterative approach using a 2-km moving window. A Bayesian hydrometeor classification algorithm is also adopted to support the analysis of the storm characteristics. Extemporaneous signal extinction caused by close-range hail core causing significant differential phase shift in very short range path is documented. Nevertheless, the localized and nearby peak of precipitation amount was very well reconstructed using a combined polarimetric rainfall algorithm based on RSD measurements in California by Matrosov et al.(2005).

* *Corresponding author address:* Gianfranco Vulpiani, Presidency of the Council of Ministers, Department of Civil Protection, Rome, Italy;
email: gianfranco.vulpiani@protezionecivile.it

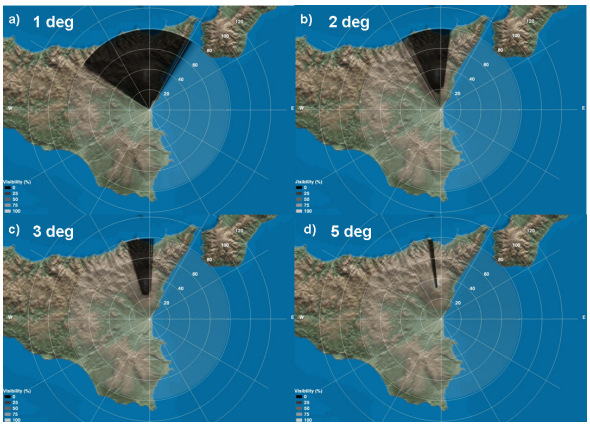

Figure 1: Visibility maps of the considered radar system at 1, 2, 3 and 5 deg antenna elevation, respectively.

2. RADAR SYSTEM AND DATA PROCESSING

The considered system is a SELEX-Gematronik 50 DX polarimetric radar with a 3-dB beam width of 1.3 ° and 50 kW of transmit peak power. The radar was deployed at the airport of Catania by the end of 2010 and is currently integrated as gap filler within the national radar network, either for weather or volcanic ash cloud monitoring (Marzano et al., 2013). The operational observation strategy, repeated every 10 minutes, includes 12 PPI sweeps used for rainfall estimation, with antenna elevation angle ranging from 1 to 21.6 degrees, and a vertical-incidence scan used for Z_{DR} calibration. The adopted PRF is 1875 Hz, which corresponds to a maximum unambiguous range of 80 km, while the range resolution is 200 m.

Due to the presence of the Etna volcano, whose peak (about 3.2 km above sea level) is located at about 30 km north from the radar, a wide azimuth sector (about 90 degree) is shielded at low elevation scans, as depicted in Figure 1. At 3 deg, the shielded sector shrinks to about 20 deg of width, becoming almost negligible at 5 deg. The main steps of the applied processing chain, i.e., differential phase processing, attenuation correction and rainfall estimation, are detailed in the following subsections.

2.1 Differential phase processing

The iterative moving-window range derivative approach proposed in Vulpiani et al. (2012) is applied in the present work. This methodology enables, on one side, to easily remove the offset on Φ_{DP}, facilitating the application of any attenuation correction procedures, and, on the other side, to control the expected K_{DP} standard deviation, expressible as follows

$$\sigma\left(K_{DP}^{(I)}\right)=\frac{1}{\sqrt{2N^{I}}}\frac{\sigma\left(\Psi_{DP}\right)}{L} \quad (1)$$

where I is the number of iterations (with $I \geq 1$), N the number of range gates contained in the moving window of length L (km), and Ψ_{DP} is the measured differential phase, i.e., the sum of the differential propagation (Φ_{DP}) and backscatter phase (δ_{HV}).

In this work, a 2-km moving window was applied within a threefold iteration scheme (i.e., I=3).

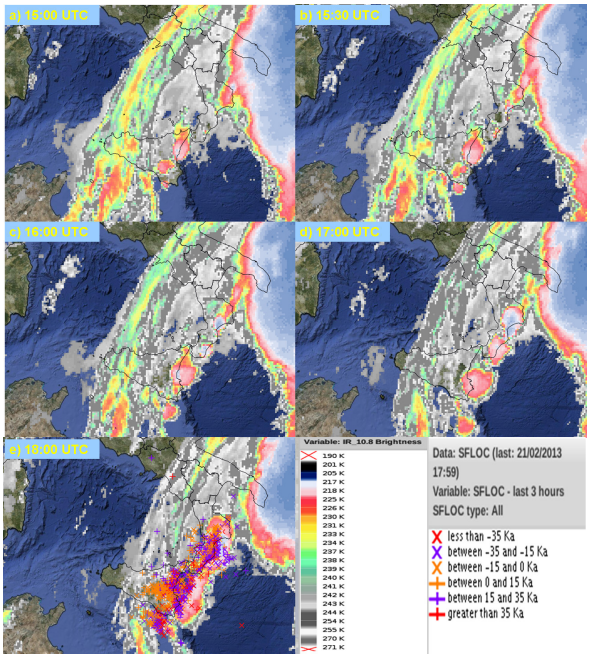

Figure 2: Brightness temperature (° K) retrieved by the 9th channel (IR10.8 μm) of the SEVIRI sensor on board of the geostationary MSG EUMETSAT satellite. Panels e) shows the superposition of the BT at 1800 UTC and the lightning registered in the previous 3 hours.

2.2 Attenuation correction

Two methodologies for compensating attenuation are applied in the present study, both assuming a linear relationship between specific attenuation (α_H), specific differential attenuation (α_{DP}) and specific differential phase, i.e., $\alpha_{H,DP}=\gamma_{H,DP}\ K_{DP}$.

The first, based on the findings of Matrosov et al. (2005) and denoted as MA05, assumes γ_H=0.25 dB deg^{-1} and γ_{DP}=0.033 dB deg^{-1}. These coefficients were obtained through scattering simulations based on RSD observations collected on the Pacific coastline of California during the Hydrometeorological Testbed (HMT-04) between December 2003 and March 2004.

Because climatology of southern Italy (including Sicily) and the coastal area of California are similar, according to the Köppen-Geiger climate classification (Kottek et al., 2006), we assume that these coefficients can be applied to our case. The second considered attenuation correction algorithm, proposed in Vulpiani et al. (2008) and named APDP, attempts to optimize $\gamma_{H,DP}$ with respect to the DSD variability of particles along the path. In this light, a Bayesian hydrometeor classification approach, adapted from Marzano et al. (2008) is applied. The APDP procedure can be summarized through the following few steps:

i. a preliminary attenuation correction is performed assuming a $\gamma_{H,DP}$ constant as in MA05. At this stage the temperature profile (T), retrieved from the closest available radio sounding, is used to roughly discriminate rain from frozen particles;
ii. the corrected $Z_{H,DR}$ are then used with K_{DP}, ρ_{HV} and T for hydrometeor classification;
iii. values of $\gamma_{H,DP}$ are associated to each rain type (i.e., light, moderate, heavy, large drops) as derived from scattering simulations (Vulpiani et al. 2008);
iv. at each range distance r an optimal $\gamma^{opt}_{H,DP}(r)$ is computed as the weighted average of the retrieved path-distributed $\gamma_{hh,dp}$, i.e., $\gamma^{opt}_{H,DP}(r)=\int_0^r K_{DP}(s)\ \gamma_{H,DP}(s)ds \Big/ \int_0^r \gamma_{H,DP}(s)ds$;
v. $Z_{H,DR}$ are finally corrected as

$$Z_{H,DR}(r)=Z^{m}_{H,DR}(r)+2\int_0^r \gamma^{opt}_{H,DP}(s)\ K_{DP}(s)\ ds \quad (2)$$

where $Z^{m}_{H,DR}$ represents the measured reflectivity and differential reflectivity, respectively.

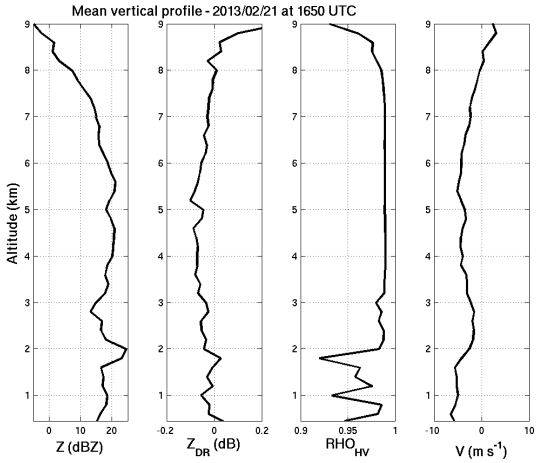

Figure 3: Mean vertical profiles of Z (dBZ), Z_{DR} (dB), ρ_{HV}, and Doppler velocity V (m s^{-1}) collected observing stratiform precipitation at vertical incidence on the 21st February 2013 at 1650 UTC.

2.3 Rainfall estimation

Specific differential phase is known to be immune to attenuation, provided the signal is not extinguished, calibration and partial beam blocking. Nevertheless, K_{DP} is sensitive to noise, especially for low precipitation regimes. For this reason, K_{DP} is typically used in combination with Z and Z_{DR} for rainfall estimation.

In the present work we applied a combined algorithm of the form of a weighted sum to avoid discontinuities introduced by threshold-based approaches

$$R_C = w_K \cdot R_K + (1-w_K)\cdot R_Z \quad (3)$$

where R_Z and R_K are the rainfall estimates obtained using Z (capped at 55 dBZ) and K_{DP}, respectively, through the power laws by Matrosov et al. (2005).

Assuming a conservative approach, the weight w_K is defined in such a way that R_K is considered not reliable for K_{DP} lower than 0.5 deg

km^{-1}, partially reliable in the range $0.5 \le K_{DP} < 1$ and fully reliable for $K_{DP} \ge 1.0$ deg km^{-1}:

$$w_K = \begin{cases} 0 & \text{for } K_{DP} \le 0.5 \\ 2 \cdot K_{DP} - 1 & \text{for } 0.5 < K_{DP} < 1 \\ 1 & \text{for } K_{DP} \ge 1 \end{cases} . \quad (4)$$

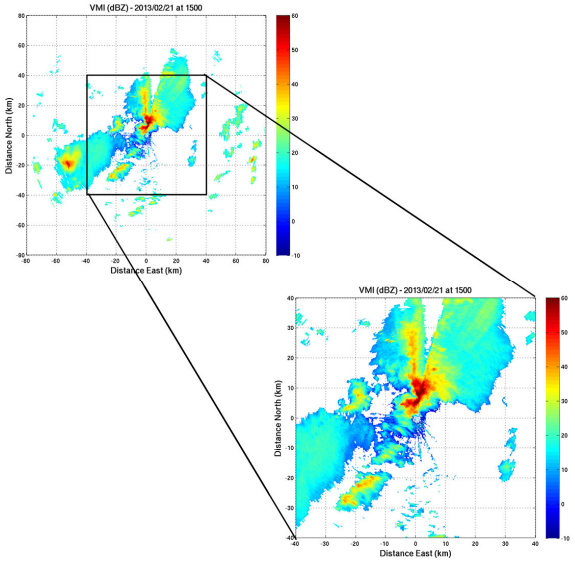

Figure 4: Vertical Maximum Intensity (dBZ) observed on the 21st February 2013 at 1500 UTC.

3. CASE STUDY

On the 21st of February 2013 an intense convective cell originated in northeastern Sicily (Italy), flash flooded the city of Catania (central-eastern coast). As it can be seen from Figure 2, showing the brightness temperature at 10.8 μm observed by the SEVIRI sensor on board of the geostationary EUMETSAT MSG satellite, the supercell lasted more than 3 hours and was also characterized by intense lightning, as shown on panel e). According, to press reports liquid precipitation was also accompanied by hail.

Fortunately, the storm developed mainly on sea causing only localized effects on the ground. Indeed, the rain gauge located in Catania registered about 60 mm in 1 hour between 15:00 and 16:00 UTC and about 70 mm in 1 and half hour. Whereas precipitation observed by nearby stations did not exceed 20 mm in 3 hours.

According to the closest available radiosounding launched from Trapani, located about 230 km far from Catania on the west of Sicily, the Freezing Layer Height was about 2 km at 1200 UTC. At 1650 UTC the stratiform tail of storm passed above the radar site, making possible the retrieval of the vertical structure. Figure 3 shows the corresponding mean vertical profiles of Z (dBZ), Z_{DR} (dB), ρ_{HV}, and Doppler velocity V.

Looking at vertical profiles of Z, ρ_{HV}, Z_{DR} and V it is possible to approximately locate the melting layer between 1.7 and 2.2 km of altitude, the latter representing the FLH. In particular, the vertical profile of V shows the increasing velocity of melting snow at decreasing altitudes down to about 1.7 km, where water drops assume a fall speed of about 5 m s^{-1}. Finally, looking at the vertical profile of the Z_{DR} we can safely state that it is fairly well calibrated.

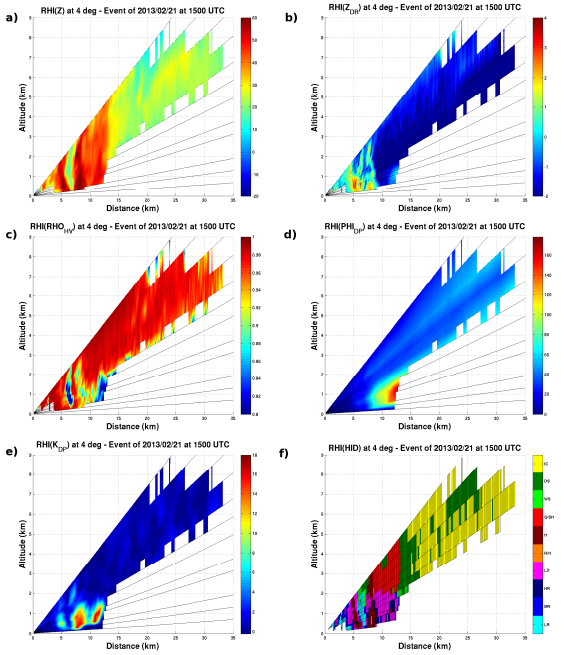

Figure 5: Pseudo RHIs of the polarimetric variables and the corresponding hydrometeor types (lower right panel) observed on the 21st February 2013 at 1500 UTC, relatively to the 4-deg azimuth angle.

4. POLARIMETRIC RADAR OBSERVATIONS

The observed supercell reached the maximum intensity overland between 1500 and 1600 UTC. Figure 4 shows the Vertical Maximum Intensity (VMI) corrected for attenuation through the MA05 technique, at 1500 UTC, when a strong convective core approached the city of Catania. An apparently shielded sector is clearly visible in the north-north-eastern direction.

However, in that direction the radar visibility is good starting from 2 deg of antenna elevation, as shown in Figure 1. The measured (attenuated) reflectivity reached almost 60 dBZ at about 5 km from the radar, while the return "disappeared" at the lowest antenna elevation angles at about 13 km from the radar. This was likely related to strong attenuation effects and not to partial beam blocking. To confirm this hypothesis, pseudo RHIs of the polarimetric observables and the corresponding hydrometeor types are examined in Figure 5 relatively to the 4-deg azimuth angle. As in Figure 4, Z and Z_{DR} are corrected for attenuation with the MA05 algorithm. Looking at Z and K_{DP}, shown on panel a) and e), 3 convective cores are identifiable at about 5, 8 and 12 km, respectively. The differential reflectivity is relatively high within the first core, exceeding 3 dB, while the correlation coefficient drops down to about 0.95. These signatures might be compatible with the presence of large drops (LD) and melting hail (H), as identified by the adopted hydrometeor classification scheme. The signature of hail or rain-hail mixture is still noticeable within second convective core, still characterized by reflectivity exceeding 60 dBZ but with higher K_{DP} (about 15 deg km^{-1}) and slightly lower Z_{DR} and ρ_{HV}. The increase in K_{DP} might be symptomatic of higher water fraction within the rain-hail mixture or hail water coat thickness.

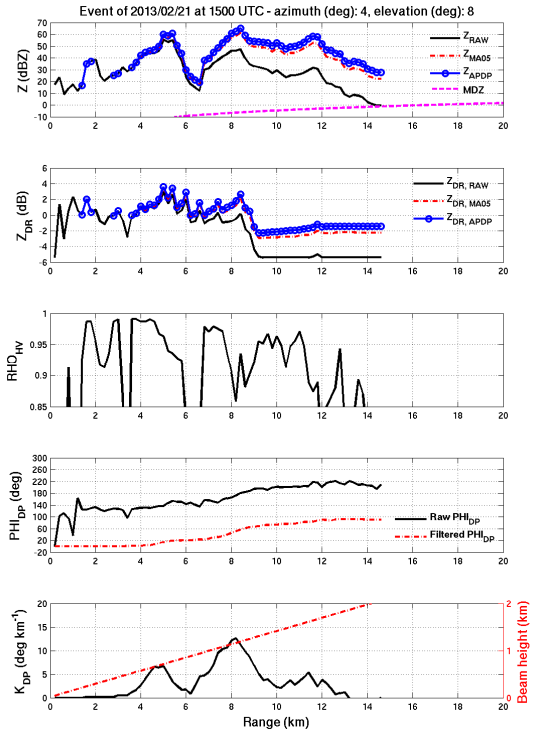

Figure 6 Range plots of the polarimetric variables and the corresponding hydrometeor types observed on the 21st February 2013 at 1500 UTC, relatively to 4-deg azimuth angle and 6 deg of antenna elevation.

However, the moderate value of Z_{DR} (about 1dB) could be related to uncompensated attenuation.

At low elevation angles, after the third convective cell, the radar signal abruptly "disappeared". This is clearly visible on Figure 6 showing the range plots of the polarimetric observables at 6 deg of antenna elevation. The measured reflectivity is shown on the upper panel together with Z corrected with MA05 and APDP. The Minimum Detectable Z (MDZ) is also superimposed.

It can be noticed that the measured reflectivity drops down at about 13 km from the radar, assuming values close to the MDZ. The data were rejected at signal processor level. The effects of decreasing SNR caused by attenuation are also traceable by the decrease of the correlation coefficient. It is also noticeable that, because the dynamic range of Z_{DR} was set by default between -5 and 15 dB, Z_{DR} reached the bottom scale at about 9 km assuming, thereafter, a plateau-like profile. Consequently, the corrected Z_{DR} profiles appear unrealistic. For this specific ray, the PIA estimated by APDP exceeded by about 10 dB the one retrieved by MA05. Comparing the raw and reconstructed Φ_{DP} profiles, we may notice that the remarkable phase shift (about 160 deg within a path of 9 km) is well reconstructed.

Figure 7, shows the pseudo-RHIs at 1530 UTC relatively to the azimuth 48 deg. A single convective cell is distinguishable in the range between 3 and 7 km from the radar. The innermost area is characterized by high values of Z, Z_{DR} and K_{DP} whose maximum values reached about 60 dBZ, 3 dB and 13 deg km^{-1}, respectively. The corresponding value of ρ_{HV} dropped down to about 0.92. Again, the polarimetric signatures are compatible with the presence of rain-hail mixture, as identified by the hydrometeor classification algorithm.

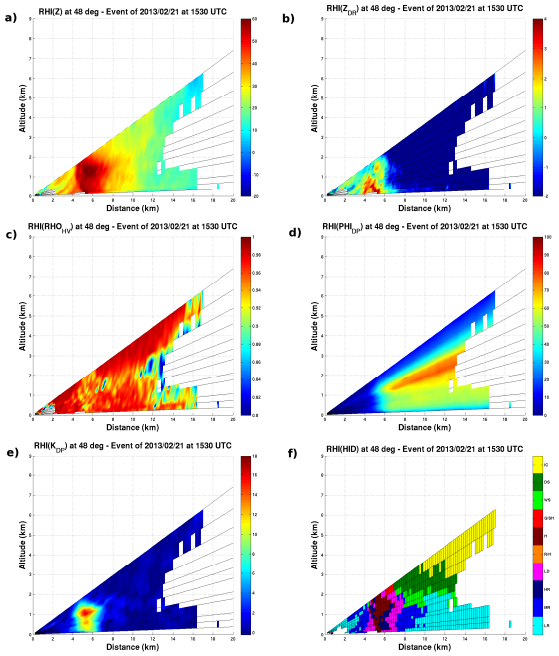

Figure 7: As in Figure 5 but relatively to the 48-deg azimuth angle at 1530 UTC.

The signal extinction likely manifested at about 13 km from the radar, as it can be inferred from Figure 8 by comparing the measured reflectivity and the MDZ. The considered correction techniques were not able to adequately compensate attenuation, especially differential attenuation. Indeed, only about 2 dB of attenuation in place of 5 dB, at least, have been estimated, the retrieved Z_{DR} being as low as -3 dB after the convective core.

Finally, the cumulated radar rainfall field obtained using the combined polarimetric algorithm is shown on Figure 9, relatively to the period 15:00-17:00 UTC. The peak of the precipitation field retrieved over ground is very close to the radar site. The nearby raingauge, located in Catania at about 6 km from the radar, registered about 60 mm in 1 hour and about 71 in 1 and a half hour.

The relative performance of the considered algorithms (i.e. R_Z, R_K, R_C) is quantitatively evaluated in terms of the following scores: $\langle\varepsilon\rangle = \langle R_R - R_G \rangle$, $\sigma_\varepsilon = (\langle(R_R - R_G)^2\rangle)^{1/2}$, Bias = $\langle R_R \rangle / \langle R_G \rangle$, FSE=RMSE/$\langle R_G \rangle$, the symbol $\langle\ \rangle$ denoting the average operator. The error indicators are summarized in Table 1.

They outline, on one side, the improvement obtained through the use of the combined polarimetric algorithm (R_C) with respect to the canonical R-Z relationship either in terms of RMSE (and FSE) or in terms of Bias. On the other side, it can be noticed that R_K outperforms R_C in terms of bias although the RMSE is higher due to the larger error standard deviation, i.e., σ_ε.

	$\langle\varepsilon\rangle$	σ_ε	RMSE	FSE	Bias
R_Z	-1.62	2.12	2.65	0.64	0.61
R_K	-0.36	2.64	2.63	0.64	0.91
R_C	-0.81	2.16	2.28	0.55	0.80

Table 1: Error scores summarizing the performance of the considered radar rainfall algorithms.

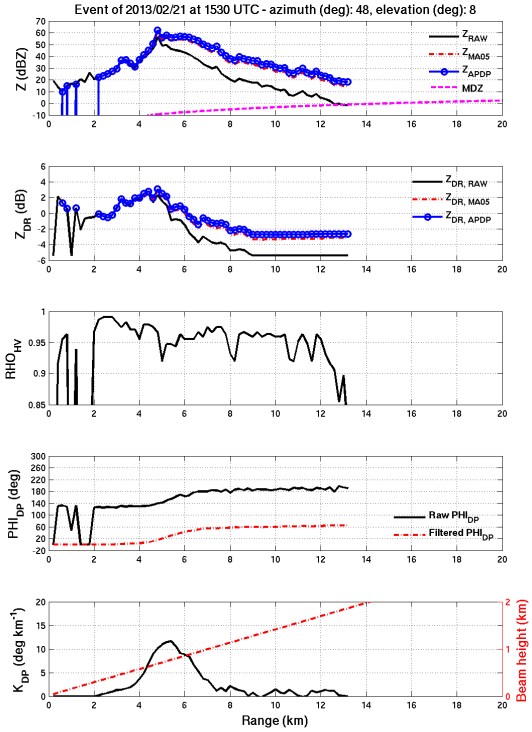

Figure 8: As in Figure 6 but relatively to the 48-deg azimuth angle at 1530 UTC and 8 deg of antenna elevation.

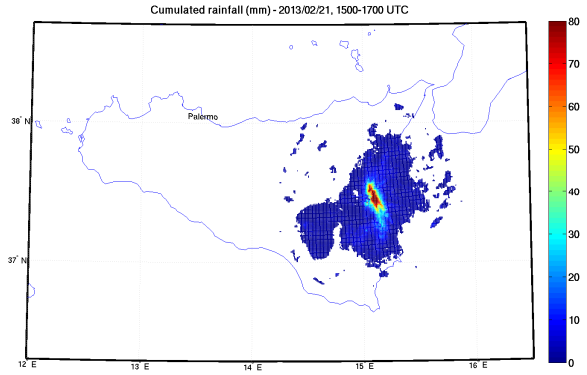

Figure 9 Polarimetric radar estimate of cumulated precipitation between 1500 and 1700 UTC on the 21st February 2013.

CONCLUSIONS

This work documented the observation, by means of an operational dual-polarized X-band radar, of a severe precipitation event that, originated in the Mediterranean sea, hit marginally the eastern coast of Sicily (Italy) causing the flash flood of Catania on the 21st of February 2013. In addition to the 60 mm of rainfall registered in 1 hour (with about 70 mm in 1 and ½ hour), the supercell originated hail as well, according to press reports. The analysis of the polarimetric observables seems to confirm the presence of melting hail justifying the huge differential phase shift observed in very short path length as well as critical attenuation and differential attenuation. The use of standard technique for attenuation compensation and a combined polarimetric rainfall algorithm enabled to carefully reconstruct the precipitation field.

REFERENCES

Anagnostou, M. N., E. N. Anagnostou, G. Vulpiani, M. Montopoli, F. S. Marzano, and J. Vivekanandan, 2008: Evaluation of X-band polarimetric radar estimates of drop size distributions from coincident S-band polarimetric estimates and measured raindrop spectra. *IEEE Trans. Geosci. Rem. Sens.*, vol. 46, N. 10, 3067-3075.

Anagnostou, M. N., J. Kalogiros, E. N. Anagnostou, M Tarolli, A. Papadopoulus, M. Borga, 2010: Performance evaluation of high-resolution rainfall estimation by X-band dual-polarization radar for flash flood applications in mountainous basins. *J. Jydrol.*, vol 394, 4-16.

Bringi, V. N., V. Chandrasekar, Polarimetric Doppler Weather Radar, 2001. Cambridge, U.K.: Cambridge Univ. Press., pp 636.

Kottek, M., J. Grieser, C. Beck, B. Rudolf, and F. Rubel, 2006: World Map of the Köppen-Geiger climate classification updated. *Meteorol. Z.*, vol. 15, N. 3, 259-263.

Junyent F., V. Chandrasekar, 2009: Theory and characterization of weather radar network, *J. Atmos. Oceanic Technol.,* 26, 474-491.

Matrosov, S. Y., D. E. Kingsmill, B. E. Martner, 2005: The utility of X-band polarimetric radar for quantitative estimates of rainfall parameters. *J. Hydrom.*, vol. 6, 248-262.

Matrosov, S. Y., R. Cifelli, D. Gochis, 2013: Measurents of heavy convective rainfall in the presence of hail in flood-prone areas using an X-band polarimetric radar. *J. Appl. Meteor and Clim.*, vol. 52, N. 2, 395-407.

Marzano, F. S., D. Scaranari, M. Montopoli, and G. Vulpiani, 2008: Supervised classification and estimation of yydrometeors from C-band dual-polarized radars: a Bayesian approach. *IEEE Trans. Geosci. Rem. Sens.*, vol. 46, N. 1, 85-98;

Marzano, F.S., M. Montopoli, E. Picciotti, G. Vulpiani, 2013: Inside Volcanic clouds. Remote Sensing of Ash Plumes Using Microwave Weather Radars. Bull. Amer. Meteor. Soc., in press, doi: 10.1175/BAMS-D-11-00160.1;

Rasmussen, R. M., and A. J. Heymsfield, 1987: Melting and shedding of graupel and hail. Part 1: Model physics. *J. Atmos. Sci.*, 44, 2754–2763.

Tabary, P., G. Vulpiani, J. J. Gourley, A. J. Illingworth, R. J. Thompson and O. Bousquet, 2009: Unusually high differential attenuation at C-band: results from a two-year analysis of the French Trappes polarimetric radar data, *J. Appl. Meteor and Clim.*, vol. 48, N.10, 2037–2053.

Vulpiani, G., P. Tabary, J. Parent-du-Chatelet, F. S. Marzano, 2008: Comparison of advanced radar polarimetric techniques for operational attenuation correction at C band. *J. Atmos. And Oceanic Tech.*, vol. 25, 1118-1135;

Vulpiani, G., M. Montopoli, L. Delli Passeri, A. Gioia, P. Giordano and F. S. Marzano, 2012: On the use of dual-polarized C-band radar for operational rainfall retrieval in mountainous areas. *J.* Appl. Meteor and Clim., vol. 51, N. 2, 405-425.

Wang, Y., V. Chandrasekar, 2010: Quantitative Precipitation Estimation in the CASA X-band Dual-Polarization Radar Network. *J. Atmos. Oceanic Technol.*, 27, 1665–1676.